Measurement of the Bottom-Quark Production Cross Section Using Semileptonic Decay Electrons in $p\bar{p}$ Collisions at $\sqrt{s} = 1.8$ TeV

F. Abe,[12] M. Albrow,[6] D. Amidei,[15] C. Anway-Wiese,[3] G. Apollinari,[23] M. Atac,[6] P. Auchincloss,[22] M. Austern,[13] P. Azzi,[17] A. R. Baden,[8] N. Bacchetta,[16] W. Badgett,[15] M. W. Bailey,[21] A. Bamberger,[6,*] P. de Barbaro,[22] A. Barbaro-Galtieri,[13] V. E. Barnes,[21] B. A. Barnett,[11] G. Bauer,[14] T. Baumann,[8] F. Bedeschi,[20] S. Behrends,[2] S. Belforte,[20] G. Bellettini,[20] J. Bellinger,[28] D. Benjamin,[27] J. Benlloch,[14] J. Bensinger,[2] A. Beretvas,[6] J. P. Berge,[6] S. Bertolucci,[7] K. Biery,[10] S. Bhadra,[9] M. Binkley,[6] D. Bisello,[17] R. Blair,[1] C. Blocker,[2] A. Bodek,[22] V. Bolognesi,[20] A. W. Booth,[6] C. Boswell,[11] G. Brandenburg,[8] D. Brown,[8] E. Buckley-Geer,[6] H. S. Budd,[22] G. Busetto,[17] A. Byon-Wagner,[6] K. L. Byrum,[1] C. Campagnari,[6] M. Campbell,[15] A. Caner,[6] R. Carey,[8] W. Carithers,[13] D. Carlsmith,[28] J. T. Carroll,[6] R. Cashmore,[6,*] A. Castro,[17] Y. Cen,[18] F. Cervelli,[20] K. Chadwick,[6] J. Chapman,[15] G. Chiarelli,[7] W. Chinowsky,[13] S. Cihangir,[6] A. G. Clark,[6] M. Cobal,[20] D. Connor,[18] M. Contreras,[4] J. Cooper,[6] M. Cordelli,[7] D. Crane,[6] J. D. Cunningham,[2] C. Day,[6] F. DeJongh,[6] S. Dell'Agnello,[20] M. Dell'Orso,[20] L. Demortier,[23] B. Denby,[6] P. F. Derwent,[15] T. Devlin,[24] D. DiBitonto,[25] M. Dickson,[22] R. B. Drucker,[13] K. Einsweiler,[13] J. E. Elias,[6] R. Ely,[13] S. Eno,[4] S. Errede,[9] A. Etchegoyen,[6,*] B. Farhat,[14] M. Frautschi,[16] G. J. Feldman,[8] B. Flaugher,[6] G. W. Foster,[6] M. Franklin,[8] J. Freeman,[6] H. Frisch,[4] T. Fuess,[6] Y. Fukui,[12] A. F. Garfinkel,[21] A. Gauthier,[9] S. Geer,[6] D. W. Gerdes,[15] P. Giannetti,[20] N. Giokaris,[23] P. Giromini,[7] L. Gladney,[18] M. Gold,[16] J. Gonzalez,[18] K. Goulianos,[23] H. Grassmann,[17] G. M. Grieco,[20] R. Grindley,[10] C. Grosso-Pilcher,[4] C. Haber,[13] S. R. Hahn,[6] R. Handler,[28] K. Hara,[26] B. Harral,[18] R. M. Harris,[6] S. A. Hauger,[5] J. Hauser,[3] C. Hawk,[24] T. Hessing,[25] R. Hollebeek,[18] L. Holloway,[9] A. Hölscher,[10] S. Hong,[15] G. Houk,[18] P. Hu,[19] B. Hubbard,[13] B. T. Huffman,[19] R. Hughes,[22] P. Hurst,[8] J. Huth,[6] J. Hylen,[6] M. Incagli,[20] T. Ino,[26] H. Iso,[26] H. Jensen,[6] C. P. Jessop,[8] R. P. Johnson,[6] U. Joshi,[6] R. W. Kadel,[13] T. Kamon,[25] S. Kanda,[26] D. A. Kardelis,[9] I. Karliner,[9] E. Kearns,[8] L. Keeble,[25] R. Kephart,[6] P. Kesten,[2] R. M. Keup,[9] H. Keutelian,[6] D. Kim,[6] S. B. Kim,[15] S. H. Kim,[26] Y. K. Kim,[13] L. Kirsch,[2] K. Kondo,[26] J. Konigsberg,[8] K. Kordas,[10] E. Kovacs,[6] M. Krasberg,[15] S. E. Kuhlmann,[1] E. Kuns,[24] A. T. Laasanen,[21] S. Lammel,[3] J. I. Lamoureux,[28] S. Leone,[20] J. D. Lewis,[6] W. Li,[1] P. Limon,[6] M. Lindgren,[3] T. M. Liss,[9] N. Lockyer,[18] M. Loreti,[17] E. H. Low,[18] D. Lucchesi,[20] C. B. Luchini,[9] P. Lukens,[6] P. Maas,[28] K. Maeshima,[6] M. Mangano,[20] J. P. Marriner,[6] M. Mariotti,[20] R. Markeloff,[28] L. A. Markosky,[28] J. Matthews,[16] R. Mattingly,[2] P. McIntyre,[25] A. Menzione,[20] E. Meschi,[20] T. Meyer,[25] S. Mikamo,[12] M. Miller,[4] T. Mimashi,[26] S. Miscetti,[7] M. Mishina,[12] S. Miyashita,[26] Y. Morita,[26] S. Moulding,[23] J. Mueller,[24] A. Mukherjee,[6] T. Muller,[3] L. F. Nakae,[2] I. Nakano,[26] C. Nelson,[6] D. Neuberger,[3] C. Newman-Holmes,[6] J. S. T. Ng,[8] M. Ninomiya,[26] L. Nodulman,[1] S. Ogawa,[26] R. Paoletti,[20] V. Papadimitriou,[6] A. Para,[6] E. Pare,[8] S. Park,[6] J. Patrick,[6] G. Pauletta,[20] L. Pescara,[17] G. Piacentino,[20] T. J. Phillips,[5] F. Ptohos,[8] R. Plunkett,[6] L. Pondrom,[28] J. Proudfoot,[1] G. Punzi,[20] D. Quarrie,[6] K. Ragan,[10] G. Redlinger,[4] J. Rhoades,[28] M. Roach,[27] F. Rimondi,[6,*] L. Ristori,[20] W. J. Robertson,[5] T. Rodrigo,[6] T. Rohaly,[18] A. Roodman,[4] W. K. Sakumoto,[22] A. Sansoni,[7] R. D. Sard,[9] A. Savoy-Navarro,[6] V. Scarpine,[9] P. Schlabach,[8] E. E. Schmidt,[6] O. Schneider,[13] M. H. Schub,[21] R. Schwitters,[8] G. Sciacca,[20] A. Scribano,[20] S. Segler,[6] S. Seidel,[16] Y. Seiya,[26] G. Sganos,[10] M. Shapiro,[13] N. M. Shaw,[21] M. Sheaff,[28] M. Shochet,[4] J. Siegrist,[13] A. Sill,[22] P. Sinervo,[10] J. Skarha,[11] K. Sliwa,[27] D. A. Smith,[20] F. D. Snider,[11] L. Song,[6] T. Song,[15] M. Spahn,[13] A. Spies,[11] P. Sphicas,[14] R. St. Denis,[8] L. Stanco,[6,*] A. Stefanini,[20] G. Sullivan,[4] K. Sumorok,[14] R. L. Swartz, Jr.,[9] M. Takano,[26] K. Takikawa,[26] S. Tarem,[2] F. Tartarelli,[20] S. Tether,[14] D. Theriot,[6] M. Timko,[27] P. Tipton,[22] S. Tkaczyk,[6] A. Tollestrup,[6] J. Tonnison,[21] W. Trischuk,[8] Y. Tsay,[4] J. Tseng,[11] N. Turini,[20] F. Ukegawa,[26] D. Underwood,[1] S. Vejcik III,[15] R. Vidal,[6] R. G. Wagner,[1] R. L. Wagner,[6] N. Wainer,[6] R. C. Walker,[22] J. Walsh,[18] G. Watts,[22] T. Watts,[24] R. Webb,[25] C. Wendt,[28] H. Wenzel,[20] W. C. Wester III,[13] T. Westhusing,[9] S. N. White,[23] A. B. Wicklund,[1] E. Wicklund,[6] H. H. Williams,[18] B. L. Winer,[22] J. Wolinski,[25] D. Y. Wu,[15] X. Wu,[20] J. Wyss,[17] A. Yagil,[6] K. Yasuoka,[26] Y. Ye,[10] G. P. Yeh,[6] J. Yoh,[6] M. Yokoyama,[26] J. C. Yun,[6] A. Zanetti,[20] F. Zetti,[20] S. Zhang,[15] W. Zhang,[18] and S. Zucchelli[6,*]

(CDF Collaboration)

[1]*Argonne National Laboratory, Argonne, Illinois 60439*
[2]*Brandeis University, Waltham, Massachusetts 02254*
[3]*University of California at Los Angeles, Los Angeles, California 90024*
[4]*University of Chicago, Chicago, Illinois 60637*

0031-9007/93/71(4)/500(5)$06.00

[5]Duke University, Durham, North Carolina 27706
[6]Fermi National Accelerator Laboratory, Batavia, Illinois 60510
[7]Laboratori Nazionali di Frascati, Istituto Nazionale di Fisica Nucleare, Frascati, Italy
[8]Harvard University, Cambridge, Massachusetts 02138
[9]University of Illinois, Urbana, Illinois 61801
[10]Institute of Particle Physics, McGill University, Montreal, and University of Toronto, Toronto, Canada
[11]The Johns Hopkins University, Baltimore, Maryland 21218
[12]National Laboratory for High Energy Physics (KEK), Tsukuba-gun, Ibaraki-ken, Japan
[13]Lawrence Berkeley Laboratory, Berkeley, California 94720
[14]Massachusetts Institute of Technology, Cambridge, Massachusetts 02139
[15]University of Michigan, Ann Arbor, Michigan 48109
[16]University of New Mexico, Albuquerque, New Mexico 87131
[17]Università di Padova, Istituto Nazionale di Fisica Nucleare, Sezione di Padova, I-35131 Padova, Italy
[18]University of Pennsylvania, Philadelphia, Pennsylvania 19104
[19]University of Pittsburgh, Pittsburgh, Pennsylvania 15260
[20]Istituto Nazionale di Fisica Nucleare, University and Scuola Normale Superiore of Pisa, I-56100 Pisa, Italy
[21]Purdue University, West Lafayette, Indiana 47907
[22]University of Rochester, Rochester, New York 15627
[23]Rockefeller University, New York, New York 10021
[24]Rutgers University, Piscataway, New Jersey 08854
[25]Texas A&M University, College Station, Texas 77843
[26]University of Tsukuba, Tsukuba, Ibaraki 305, Japan
[27]Tufts University, Medford, Massachusetts 02155
[28]University of Wisconsin, Madison, Wisconsin 53706
(Received 20 April 1993)

We present measurements of the bottom-quark production cross sections in $p\bar{p}$ collisions at $\sqrt{s}=1.8$ TeV. From the inclusive electron production rate, we have determined the bottom-quark production cross sections to be 1010 ± 270, 168 ± 43, 37 ± 10 nb for the rapidity range of $|y^b|<1.0$ and the transverse momentum ranges of $p_T^b>15$, 23, 32 GeV/c, respectively. In addition, from the associated electron-D^0 production rate, we have determined the bottom-quark cross section to be 364 ± 80(stat) ±95(syst) nb for $|y^b|<1.0$ and $p_T^b>19$ GeV/c.

PACS numbers: 13.85.Ni, 13.85.Qk

The QCD-improved parton model provides quantitative predictions for the production of heavy quarks in hadron collisions. The short distance parton-parton cross sections are calculated through a perturbative expansion in the strong coupling constant, and then convoluted with the parton structure functions of the proton and antiproton. Calculations [1–3] in next-to-leading order have been performed, which predict large corrections to the leading order results. Comparison of these calculations with experiment can determine the importance of further higher order corrections. We report a measurement of the bottom-quark production cross sections at 1.8-TeV center-of-mass energy using semileptonic decays into electrons. A similar analysis, based on decays into muons, was first performed by the UA1 Collaboration at 0.63 TeV [4].

The data were taken in 1988–89 using the Collider Detector at Fermilab (CDF) in the Fermilab Tevatron $\bar{p}p$ collider. The CDF is described in detail elsewhere [5]. In the central region (pseudorapidity $|\eta|\leq1.0$) the central tracking chamber (CTC) provides momentum analysis for charged particles with a resolution of $\sigma p_T/p_T \simeq 0.002 p_T$, where p_T is the transverse momentum in GeV/c. Outside the coil are electromagnetic (CEM) and hadron (CHA) calorimeters which employ a projective tower geometry with a segmentation of $\Delta\phi\times\Delta\eta=15°\times0.11$. A layer of proportional chambers (CES), embedded near shower maximum in the CEM, provides a more precise measurement of electromagnetic shower profiles both in azimuth (ϕ) and beam (z) directions.

Two electron triggers with E_T thresholds of 7 and 12 GeV are used for this analysis, where E_T is the transverse energy. The corresponding integrated luminosities are 0.22 ± 0.02 and 4.2 ± 0.3 pb^{-1}, respectively. The identification of electrons uses information from both the calorimeters and the tracking chambers by requiring the following.

(a) Longitudinal profile consistent with an electron shower, i.e., less than 4% leakage energy in the CHA.

(b) Lateral shower profiles measured with the CEM [6] and the CES [7] consistent with test beam data.

(c) Association of a single high p_T track with the calorimeter shower based on position matching ($R|\Delta\phi|<1.4$ cm and $|\Delta z\sin\theta|<2$ cm on the CES plane) and energy to momentum ratio ($0.75<E/p<1.4$).

Photon conversion electrons due to detector material, as well as the Dalitz decays of π^0's, are removed by looking for oppositely charged tracks which have small open-

ing angles with the electron candidates. The remaining backgrounds are photon conversion electrons whose partners have not been found, and charged hadrons which fluctuate to produce showers similar to those of electrons. The unseen conversion background is estimated to be $(17 \pm 3)\%$, using a sample of conversion pairs identified independently with information from the vertex time projection chambers [8]. The fake hadron background is estimated to be $(17 \pm 5)\%$ from the distribution of the energy fraction in the CHA. The relative amounts of both backgrounds are approximately independent of E_T after the subtraction of W and Z decay electrons described below.

Figure 1 shows the E_T distribution of electron candidates. The number of events triggered with the 7 GeV threshold is normalized to the integrated luminosity for the sample with the 12 GeV threshold. The shoulder above 25 GeV reflects the Jacobian peak from W and Z decay electrons. W electrons are removed by cutting on missing transverse energy. Z electrons are removed by cutting on the invariant mass of the electron with other electromagnetic clusters in the event. The E_T spectrum after removing Drell-Yan and W and Z decay electrons, and subtracting residual photon conversions and charged hadrons, is also shown in Fig. 1.

Semileptonic decays of bottom and charm quarks are expected to be the dominant source of electron production. Since QCD is flavor independent, b and c quarks are expected to be produced at similar rates at high p_T. The differences in the kinematics in the quark fragmentation [9] and hadron decays, and in the electron detection efficiency, result in a relative enhancement of electrons from b quarks at high E_T. For example, Monte Carlo calculations predict that charm decay electrons would account for only 10% of the observed electrons with E_T

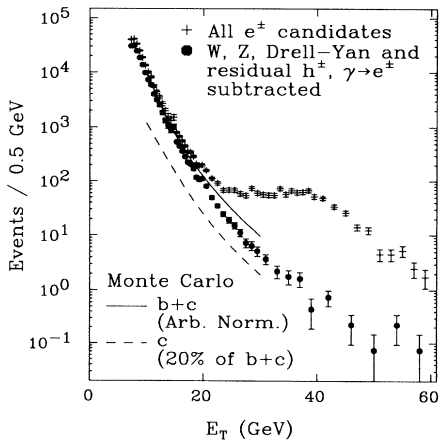

FIG. 1. The E_T spectrum of electron candidates, after removal of found conversions (crosses), and unseen conversions, fake leptons, and Drell-Yan backgrounds (points); the curves show the spectral shapes expected for $b+c$ (solid) and c alone (dashed), normalized to the data at 10 GeV.

above 10 GeV, if the bottom and charm production cross sections were equal at high p_T.

Two independent methods have been used to extract the charm fraction from the data. First, strange particles can be produced in both bottom ($b \to e^- \bar{\nu} c$, $c \to s$) and charm ($c \to e^+ \nu s$) semileptonic decays, but they have opposite charge correlations with the electron. (Throughout this Letter, a reference to a particular charge state also implies its charge conjugate state, unless otherwise stated.) We reconstruct $\bar{K}^*(892)^0 \to K^- \pi^+$, using charged particle tracks in the CTC. We observe a $\bar{K}^{*0}$ peak in the $K^- \pi^+$ pairs with electrons, as expected for the b-quark decay chain, and we observe no significant peak in $K^+ \pi^-$ pairs. We obtain an upper limit of 30% at 90% C.L. for the fraction of charm decay electrons relative to the sum of bottom and charm in the observed electron sample.

The second method uses the electron momentum component perpendicular to the jet axis, which reflects the mass of the parent hadrons and thus discriminates between bottom and charm decay electrons [4]. From the shape of this momentum spectrum, we obtain a charm fraction of $(20 \pm 10)\%$. The two methods are evidently consistent, and so we take the charm fraction to be $(20 \pm 10)\%$. Figure 1 shows the Monte Carlo spectral shapes expected for the $b+c$ and c contributions, based on the b-quark production model of Nason, Dawson, and Ellis [2].

We use the kinematic relationship between the electron and the bottom-quark spectra to obtain the bottom-quark production cross section integrated over a rapidity range $|y| < 1.0$ and over a p_T range from a threshold $p_T^{\min}$ to infinity. We use three electron E_T intervals, 10–15, 15–20, and 20–25 GeV, with corresponding b-quark $p_T^{\min}$ of 15, 23, and 32 GeV/c, respectively. The b-quark p_T thresholds are chosen so that 90% of the electrons in a given E_T interval come from b quarks of $p_T^{\min}$ and above. We use the relation

$$\sigma_b = \frac{(N_{e^-} + N_{e^+})/2}{\int \mathcal{L}\, dt\, (R_{e^-}/R_b)_{\mathrm{MC}}}, \tag{1}$$

where N_{e^-} (N_{e^+}) is the number of bottom decay electrons (positrons) observed in the data, after subtracting the fake-lepton and charm backgrounds. We have 22940 ± 2760, 2044 ± 221, 316 ± 38 electrons and positrons for the three E_T intervals, where the errors reflect the uncertainty due to the background subtraction and statistics. $\int \mathcal{L}\, dt$ is the integrated luminosity for the data. $(R_{e^-}/R_b)_{\mathrm{MC}}$ is the ratio of the electron and the b-quark rates obtained using Monte Carlo events, where R_{e^-} is the number of electrons (not including positrons) passing the same geometrical, kinematical, and identification cuts as in real data, and R_b is the number of b quarks produced in the kinematic range (p_T and rapidity). The overall factor of 2 is necessary to get the b-quark cross section (not including $\bar{b}$).

In calculating $(R_e\text{-}/R_b)_{MC}$, b-quark jets are generated with the ISAJET Monte Carlo program [10], where the b-quark p_T spectrum is slightly modified to match the calculation by Nason, Dawson, and Ellis [2]. The uncertainty in the ratio $(R_e\text{-}/R_b)_{MC}$ due to the shape of the b-quark p_T spectrum is estimated to be 8%, by comparing the electron E_T shape in the real data and Monte Carlo events. The heavy quark fragmentation is modeled with the Peterson function [11], tuned to reproduce the experimental results [9] from e^+e^- annihilation. The uncertainty in $(R_e\text{-}/R_b)_{MC}$ due to the experimental uncertainty on the fragmentation parameters (cf. Ref. [9]) is estimated to be $\pm 15\%$, essentially independent of E_T. The weak decays of nonstrange B mesons are described by the CLEO Monte Carlo program [12], where semileptonic decays employ the model by Isgur *et al.* [13]. The quantity $(R_e\text{-}/R_b)_{MC}$ includes the B hadron decay branching ratio into electrons. Although an electron can come from many stages of a B hadron decay, the primary decay $b \to e^-\bar{\nu}X$ is the predominant source of the electrons observed. We use a CLEO measurement of $\mathcal{B}(\bar{B} \to l^-\bar{\nu}X) = 0.112 \pm 0.005$ [14] for nonstrange B mesons, and assume the same value for other B hadrons. To find the electron detection efficiency, the Monte Carlo events are passed through a detector simulation based on the calorimeter response for test beam particles. The estimated electron detection efficiency is $(60 \pm 10)\%$ at 10 GeV and $(30 \pm 5)\%$ at 25 GeV. The decrease in efficiency with increasing electron E_T is due to the increased collimation of the B jet, which tends to increase both E/p and the observed CHA leakage.

The numerical values of the ratio $(R_e\text{-}/R_b)_{MC}$ are 2.82×10^{-3}, 1.53×10^{-3}, and 1.10×10^{-3} for the three electron E_T intervals. All the systematic effects in estimating the Monte Carlo cross section ratio $(R_e\text{-}/R_b)_{MC}$ are combined in quadrature with the uncertainties in the background subtraction in the electron sample, and in the luminosity measurement, to yield a 26% total systematic uncertainty. By evaluating Eq. (1) for the three electron E_T intervals, we obtain b-quark production cross sections for the rapidity range $|y^b| < 1.0$ of 1010 ± 270, 168 ± 43, and 37 ± 10 nb, for the intervals $p_T^b > 15$, 23, and 32 GeV/c, respectively.

A more direct signature for bottom production is the associated production of a charmed particle with the electron. We look for D^0, which is expected from the decay $\bar{B}_{u,d} \to e^-\bar{\nu}D^0X$. Electrons triggered with the 12 GeV threshold are used for this study. The D^0 is identified through the $K^-\pi^+$ decay, using all oppositely charged CTC track pairs, where each track is required to be within a cone of radius 0.6 in η-ϕ space around the electron. We also require the momentum of the kaon (pion) to be 1.5 (0.5) GeV/c or above. We show in Fig. 2 the invariant mass spectrum of $K\pi$ pairs. In B-meson decay the electron charge is identical to that of the kaon ("right sign" combination). We observe 68 ± 15 $D^0 \to K^-\pi^+$ decays in the right sign pairs. The signal is absent in the wrong sign pairs and in the electron sample from identified photon conversions.

From the number of D^0's we derive the number of semileptonic B decay electrons, using a CLEO measurement [15] of the combined branching ratio

$$\mathcal{B}_{eD^0} \equiv \frac{\mathcal{B}(\bar{B}_{u,d} \to D^0 X l^- \bar{\nu})}{\mathcal{B}(\bar{B}_{u,d} \to X' l^- \bar{\nu})} \mathcal{B}(D^0 \to K^-\pi^+) = 0.028 \pm 0.004 . \quad (2)$$

The D^0 reconstruction efficiency, which takes into account kinematical acceptance, track-finding efficiency, and kaon decay in the CTC, is estimated to be 0.41

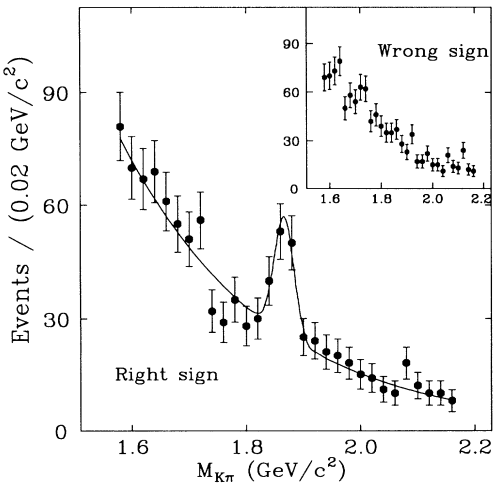

FIG. 2. $K^\pm\pi^\mp$ invariant mass distributions for right sign and (inset) wrong sign pairs.

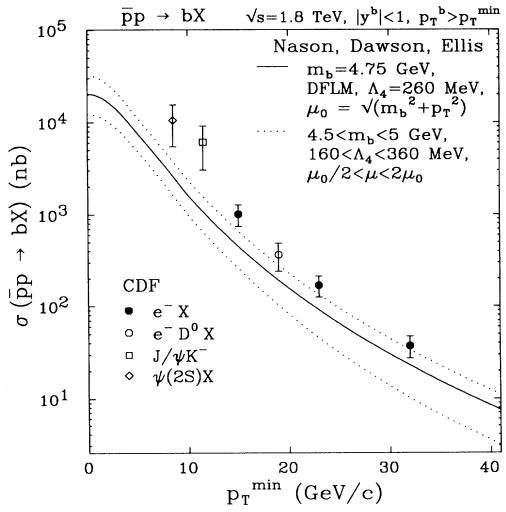

FIG. 3. The b-quark production cross sections measured using the inclusive electron rates and the e^-D^0 rate. Also shown are other CDF measurements [17,18] and the theoretical calculation by Nason, Dawson, and Ellis [2].

± 0.02, using the Monte Carlo detector simulation. In deriving the number of inclusive semileptonic B decay electrons, we take into account the small difference in electron detection efficiency between the exclusive ($\bar{B} \to e^- \bar{\nu} D^0 X$, $D^0 \to K^- \pi^+$) and the inclusive ($\bar{B} \to e^- \bar{\nu} X'$) modes. The b-quark production cross section is then derived using Eq. (1). We assume that only nonstrange B mesons contribute to the electron-D^0 signal, and so the method measures the nonstrange B-meson component of b jets. By assuming that bottom hadrons are produced with the ratio $B_u{:}B_d{:}B_s{:}B_{\text{baryon}} = 0.375{:}0.375{:}0.15{:}0.10$ [16], we find $\sigma(\bar{p}p \to bX;\ p_T^b > 19\ \text{GeV}/c,\ |y^b| < 1.0) = 364 \pm 80 \pm 95$ nb, where the first uncertainty is statistical, and the second is systematic, including 13% uncertainty in the combined branching fraction $\mathcal{B}_{eD^0}$ and other uncertainties common to the previous method.

The results are shown in Fig. 3, together with independent measurements using $B^\pm \to J/\psi K^\pm$ [17] and $\psi(2S)$ events [18]; the error bars show the statistical and systematic uncertainties combined in quadrature. We note that although the data points are statistically independent of each other, there exist common systematic uncertainties. Also shown is the theoretical calculation by Nason, Dawson, and Ellis [2] in next-to-leading order, with their estimate of the theoretical uncertainty arising from choices of the renormalization scale μ, the bottom-quark mass, and uncertainty in the proton structure through the choice of the QCD Λ parameter. The theoretical calculation is about 1.4 to 2.2 standard deviations lower than the central values for the electron data.

We thank the Fermilab staff and the technical staffs of the participating institutions for their vital contributions. This work was supported by the U.S. Department of Energy and National Science Foundation, the Italian Istituto Nazionale di Fisica Nucleare, the Ministry of Science, Culture and Education of Japan, and the A.P. Sloan Foundation.

*Visitor.

[1] P. Nason, S. Dawson, and R. K. Ellis, Nucl. Phys. **B303**, 607 (1988); G. Altarelli, M. Diemoz, G. Martinelli, and P. Nason, Nucl. Phys. **B308**, 724 (1988).
[2] P. Nason, S. Dawson, and R. K. Ellis, Nucl. Phys. **B327**, 49 (1989).
[3] W. Beenakker, H. Kuijf, W. L. van Neeven, and J. Smith, Phys. Rev. D **40**, 54 (1989); W. Beenakker *et al.*, Nucl. Phys. **B351**, 507 (1991).
[4] C. Albajar *et al.*, Phys. Lett. B **186**, 237 (1987); **213**, 405 (1988); **256**, 121 (1991).
[5] F. Abe *et al.*, Nucl. Instrum. Methods Phys. Res., Sect. A **271**, 387 (1988), and references therein.
[6] J. Proudfoot, in *Calorimetry for the Superconducting Supercollider, Alabama, 1989,* edited by R. Donaldson and M. Gilchriese (World Scientific, Singapore, 1989). We use LSHR < 0.2.
[7] F. Abe *et al.*, Phys. Rev. Lett. **68**, 2734 (1992). We use $\bar{\chi}^2 < 10$.
[8] F. Abe *et al.*, Phys. Rev. D **43**, 664 (1991).
[9] J. Chrin, Z. Phys. C **36**, 165 (1987); D. Decamp *et al.*, Phys. Lett. B **244**, 551 (1990). We use $\langle z \rangle = 0.83 \pm 0.03$ or $\epsilon = 0.006 \pm 0.002$.
[10] F. E. Paige and S. D. Protopopescu, Report No. BNL-38034, 1986 (unpublished).
[11] C. Peterson, D. Schlatter, I. Schmitt, and P. M. Zerwas, Phys. Rev. D **27**, 105 (1983).
[12] P. Avery, K. Read, and G. Trahern, Report No. CSN-212, 1985 (unpublished).
[13] N. Isgur, D. Scora, B. Grinstein, and M. Wise, Phys. Rev. D **39**, 799 (1989).
[14] S. Henderson *et al.*, Phys. Rev. D **45**, 2212 (1992).
[15] R. Fulton *et al.*, Phys. Rev. D **43**, 651 (1991).
[16] B. Adeva *et al.*, Phys. Lett. B **252**, 703 (1991); D. Decamp *et al.*, Phys. Lett. B **258**, 236 (1991).
[17] F. Abe *et al.*, Phys. Rev. Lett. **68**, 3403 (1992).
[18] F. Abe *et al.*, Phys. Rev. Lett. **69**, 3704 (1992).